Image processing through deep learning after DI extraction for the SHM of aeronautic composite structures using Lamb waves

S. Husain*[a], M. Rébillat*[b], F. Ababsa[b]
[a]École polytechnique universitaire de Sorbonne Université, Paris, France
[b]PIMM, Arts et Métiers ParisTech, CNRS, CNAM, HESAM University, Paris, France;

ABSTRACT

Structural health monitoring (SHM) is a crucial process that enables the diagnosis of the health state of civil and industrial smart structures through autonomous and in-situ non-destructive measurements. The focus of our study is on the damage classification step within the aeronautic context, where the primary objective is to distinguish between different damage types in composite plates. To achieve this, we considered three experimental damages - impact, delamination, and magnet - on an aeronautic composite plate embedded with a piezoelectric array and excited it using ultrasonic guided Lamb waves. We recorded signals resulting from pristine and damaged states and used three methods to create images from the raw recorded data. These methods employed Damage Indexes (DI) that compare signals in the healthy and damaged states for each actuator/sensor path. For the first two methods, images were directly created as pixel maps depicting DI distribution according to the actuator/receiver pairs over the plate. The last method applied the classical RAPID damage localization algorithm, generating damage localization maps associated with a given DI. The datasets generated by the two methods were fed into a Convolutional Neural Network (CNN) for damage classification purposes. Our study demonstrated that the best accuracy for the introduced methods was above 92% for different hyperparameters configurations, indicating their ability to perform the desired SHM damage classification task. The DI-based approach was much more efficient than the RAPID-based method, which was not intuitively expected. These findings contribute to the development of effective SHM techniques for aeronautic composite plates, paving the way for further improvements in this critical field.

Keywords: structural health monitoring (SHM), damage index (DI), convolutional neural network (CNN), composite structures, deep learning

1. INTRODUCTION

In the aeronautic industry, using materials that combine both lightness and robustness is essential as they represent a key to reduce the aircraft's weight but can also effectively improve the aircraft's strength and stiffness. Consisting of a matrix and a reinforcing phase, composites materials allow for high stiffness and resistance, and longue fatigue life. In this regard, composites are interesting for aeronautic applications and represent a major stake for the current and future aerospace applications. However, damage evolution and fracture behavior in composites remains a challenge work as they occur beneath the top surface and can be of different types (matrix cracking, impact damage, delamination, …). Continuously monitoring critical components is one of the solutions allowing to ensure the sustainability of the structure, mainly at the early stages of damage evolution. There are several methods that allow to identify and to monitor the damage evolution, most of which are part of Non-Destructive Testing (NDT) methodologies. Although effective, they require heavy equipment, are time consuming for large structures, and mainly involve human action. To allow for more flexibility, Structural Health Monitoring (SHM) procedures are emerging, which are focusing on investigating in real time and autonomously the health of complex structures [1]. For this to be done, embedding sensors and actuators throughout the structure has become an essential step for a SHM process. Piezoelectric elements, commonly used because of their size and cost, embedded inside the composite plies or bonded on top of composite materials during the manufacturing process. By means of Lamb waves (emitted and received by the piezoelectric elements) that will explore the entire composite structure and interact with potential damages, various sensors/actuators paths are excited to obtain damage-related information [2]. Corresponding signals are then processed and used for further monitoring applications. Damage Index (DI) that quantify the damage effect on a signal can then be computed for SHM purposes. These DIs constitutes the starting point of the present study focusing on the damage classification step. A few research works have shown that data from simulated or recorded signals could efficiently be used to train and test deep-learning algorithms for classifying damage cases in the context of the SHM of aeronautic composite structures. Machine learning techniques are very interesting in that context as they can learn the complex link between input and outputs so that reliable conclusions about structural

safety may be drown. As an example, we can cite finite elements models providing vibration data transformed into 2D data that are then fed into Convolutional neural network (CNN) [3], or raw DI datasets used in a multilayer perceptron (MLP) classifier [4], a former version of artificial neural network (ANN). ANN refers to machine learning methods that use artificial neuron schemes based on biological neural network, that train their units by adapting their weights to a current processed output to a target output. By using the error prediction, the network aims to improve its accuracy regarding a classification task. ANN has proven its efficiency for damage detection issues on civil infrastructure such as bridge, or curtain walls structures [5]. Other Machine learning solutions are implemented in the literature, such as Least-squares support vector machine (LSSVM) [6], that shows better generalization results compared to ANN for the same limited amount of data. As these methods show good results for simple structures, CNN is shown to be suited to more various complex cases, from image classification and localization applied grandstand to computer-aided detection in medicine. Therefore, CNNs can learn the optimal features and classifier parameters to achieve SHM steps and can potentially outperform conventional machine learning methods in many problems.

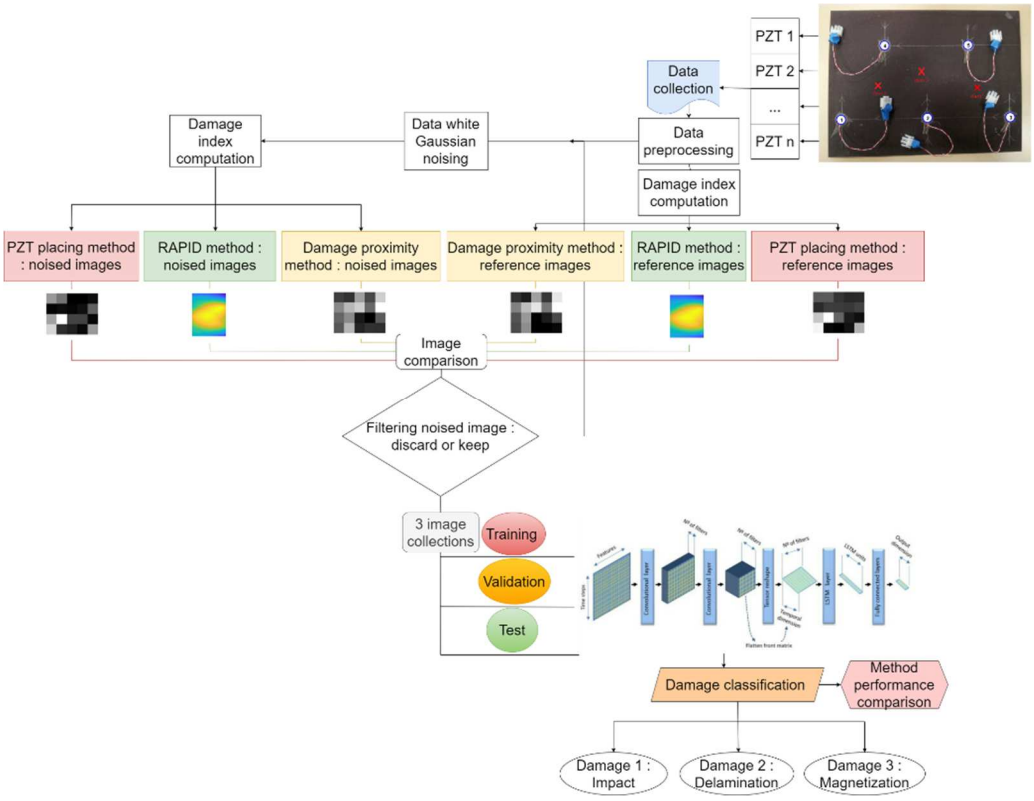

Figure 1. The work dataflow, from data acquisition and transformation into 2D images to CNN classification.

The overall dataflow of the study is presented in Figure 1. First, the received signals will be processed to compute the DIs for various tested damage configuration. For each damage case, reference images will then be generated from these DIs, while on the other hand, a white Gaussian noise will be added to the reference signals to compute a new list of DIs. "Noisy" images will then be generated from these noisy DIs and then compared with the reference images in order to keep only images that are relevant for supervised learning. The process is repeated until there are enough images to form image collections for each damage. The images are then separated into training, validation, and test bases depending on the methods, and fed into a CNN to perform a classification task. The methods will finally be compared according to their performance.

This paper objective is thus to study methods that are intuitive, easy to implement and efficient, allowing to transform raw Lamb waves signals datasets into 2D images collections through DI computation and to assess them through a CNN deep-leaning process. The layout of this paper is as follows: Section 2 details the material and the experimental setup that was used to generate and collect data experimentally on aeronautic composites structures for three different damage types (impact, delamination, magnet). Section 3 then introduces the methods that were studied for 2D images generation from DIs. These images are then fed into a CNN whose performances on a classification task are discussed in Section 4. Finally, Section 5 summarizes the main conclusions.

2. EXPERIMENTAL SETUPS AND IMAGES GENERATION METHODS

2.1 Lamb waves raw data acquisition

The experimental data used here are coming from a previous study by the same team [7]. A complex composite aeronautic plate made of composite carbon epoxy is considered (see Figure 2). It is made with 4 plies oriented along [0°/ 45°/ 45°/ 0°] and its dimension are 400x300 mm. A 5 piezoelectric elements array is used, and each element is bonded to the plate and acts sequentially as sensor and actuator in order to emit and receive Lamb waves signals. They are numbered from 1 to 5 and have a 12.5 mm radius. In the study, three types of damage (impact, delamination, magnet) are considered as shown in Figure 2.

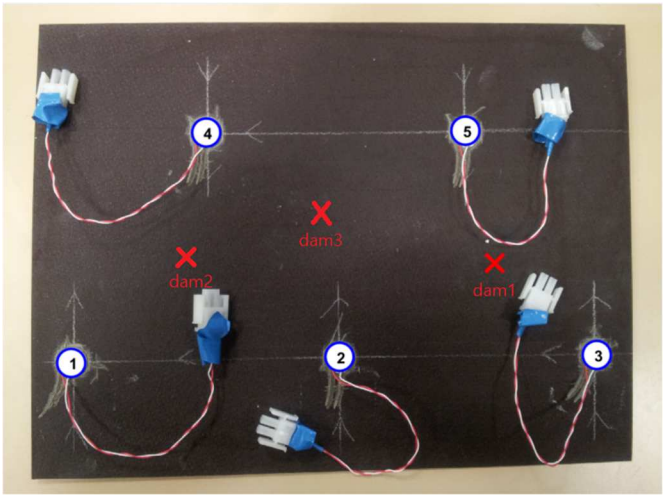

Figure 2. Epoxy plate under study, where “dam1” refers to impact, “dam”2 refers to delamination and “dam3” refers to magnet damage.

The first damage is made by an impact, the second damage is made by placing magnet from both sides of the plate, and the third damage is an artificial delamination achieved by placing a small Teflon tape between two composite plies. Lamb wave measurement process is described in detail in [7]. Lamb waves are used as they can travel across the plate and possibly interact with damages. The signals are 5 cycles “burst” with an amplitude of 10 V and a central frequency of 200 kHz. The signals collected and emitted are composed of 1000 points, with 1 MHz sample frequency. For statistical purposes, 10 repetitions are performed for each signal. Signals are preprocessed with denoising using a discrete wavelet transform that decomposes the signal to be analyzed on a “morlet” wavelet basis to retain only a certain number of coefficients of this decomposition, and time aligned with a reference pristine state because of slight subsample time misalignment that the data acquisition hardware can induce.
After each signal has been collected for all receiver-actuator pairs, damaged states signals are compared to the reference signals in order to compute 40 candidate Damage Indexes (DI) designed for damage detection. In section 5.2 of chapter 4 of his PhD thesis [8], Briand studied families of DI on several test plates each with a different fatigue scenario (delamination, impact). The objective was to compute an average score of 3 sub-scores determining the coherence, the range, and the consistency of the DIs when faced with different scenarios. It was found that the DIs based on residual energy, as well as those based on signal correlation, are the most robust in terms of the variety of scenarios, environmental conditions, and geometrical uncertainties such as the exact position of the piezoelectric sensors. For the reference-damage configurations, 100 DIs can be computed (10 healthy signals versus 10 damaged ones), compared to only 45 DIs for the ref-ref comparison configuration, because redundant comparisons within the 10 available repetitions are discarded.

2.2 Image base generation for different methods from DIs in order to feed a CNN.

In this section, we will then describe methods that aim at creating 2D images based on previously computed DIs, the data augmentation technique that has been applied to increase the number of images per dataset, and finally the CNN architecture that was chosen for classification purposes.
The methods that were developed in this study rely on the use of the DI datasets that were computed for each damage configuration. The key idea is that they use prior knowledge about the PZT positions to organize the 2D image in a manner that is coherent with respect to the acquired Lamb waves signals. For the first method, considering a damage at a given position, images are built in the following way: we place on the columns from left to right pixels related to the closest to

and farthest actuator PZT from the damage. Pixels on the rows describe the same order as the column placing, but for the receivers. For instance, a pixel located at pixel block (3,4) would describe the DI between the third closest PZT to the damage acting as actuator and the fourth closest PZT to the damage acting as receiver, excluding the actuator we placed on the column as we do not consider actuator- receiver pair for the same PZT. So, each image consists of 4-pixel blocks in a row, and 5-pixel blocks in a column. As the standard deviation of the list of 100 DIs for a sensor pair is relatively small, each pixel is set as the mean of the 100 DIs repetitions. This average DI value being between 0 and 1, the pixel values are normalized by the maximum pixel according to a grayscale. When generating images with this method, we noticed a main issue. As the DIs are supposed to describe the deformation of a reference signal between two sensors, the method of pixel arrangement implies a form of grey level gradient from left to right and from top to bottom, but this is not observed in any image. Typically, the DI of the couple closest to the damage is not the pixel at the top left of the image when it should be. Furthermore, we used prior knowledge about the damage positions, but this information is generally unavailable for a SHM study. A method that uses experimental knowledge that the operator can manipulate and that is independent of the damage would therefore be more attractive in all respects.
We turned to a method that maintains a similarity of image construction for different damages, which the CNN will be able to process, even if the position of the damages is not visually informed for an observer.
The second method, called the sensor placement (SP) method, is very similar to the previous one and uses the placing of the sensors that is consistent regardless of the damage position. Images are made in the following way: we place on the columns from left to right pixels related to the leftmost to the rightmost actuator PZT of the plate, and pixels on the rows describe the same order as the column placing, but for the receivers.
For example, a pixel located at (3,4) in the image matrix describes the DI between the third leftmost PZT of the plate acting as actuator and the fourth leftmost PZT on the plate acting as sensor, excluding the actuator we placed on the column as we do not consider actuator-receiver pair for the same PZT. The pixel values are the same as in the first method. As the physical meaning of the DIs is unchanged, we expect to see images like the damage proximity method, where the understanding of the pixel distribution is not intuitive with respect to the DI concept. Indeed, the resulting distribution of pixels is visually confusing, since a pixel does not represent a probability of damage at a given point on the plate, but a DI for a path between two sensors. But this will not represent an obstacle for learning. Indeed, although the physical meaning of the SP images is not obvious to us, images of each class do capture the spatial distribution of the sensors, which is constant over the course of the study cases. The underlying spatial information will be processed by a CNN through labelling of the learning base to discriminate the damages.

For this reason, it would be interesting to implement the Reconstruction Algorithm for the Probabilistic Inspection of Damage (RAPID) method. This one gives a natural meaning to each pixel that makes up the images, each defining the probability of the damage being present. In addition to this, RAPID methods consider the distribution of the image points with respect to the sensors, and the physical meaning of the DIs will be used to construct visually understandable images for us and the CNN. The first RAPID implementation was proposed by Zhao et al [9] in 2007. To determine the location of damage, they assume that the probability of damage being at a given point on the plate is related to the rate of signal distortion between pairs of piezoelectric sensors, as well as to the positioning of the sensors relative to the point. The expression of the probabilistic distribution will not be detailed here but can be found in reference [9]. Images generated for both methods are show in Figure 3.

In normal circumstances, the 40 available DIs would therefore provide us with 40 images per damage, which is clearly not enough to perform a supervised learning task such as a deep neural network. The network would rely too much on the training reference images and we would inevitably observe overfitting. We therefore need to apply an artificial but realistic method to generate more images from the original images. With this in mind, we chose to work with additive white Gaussian noise (AWGN), but in a different way to what is done in the literature. Indeed, the data augmentation techniques often implemented aim to work with the images in support, in order to generate new ones. We can mention flip, rotation, resizing, cropping, or adding noise directly to the source image. In our case, it will be the temporal signals that are modified. MATLAB makes it possible to add Gaussian noise directly to a signal, stored in our case in matrix. AWGN is characterized by its signal-to-noise ratio (SNR) whose expression is:

$$SNR_{dB} = 10log_{10}\left[\left(\frac{A_{signal}}{A_{bruit}}\right)^2\right] = 20log_{10}\left(\frac{A_{signal}}{A_{bruit}}\right)$$

The AWGN models random noise distributed according to a normal distribution and simulates the background noise, caused for example by interference, of a physical channel, in our case the plate, which serves as an information transmission gateway between a transmitter and a receiver. It is therefore perfectly suited for this kind of situation. This model does not consider the attenuation of the signals between the sources, but given the centimeter distance between the sensors, this

phenomenon can be neglected. Signals for the 3 damages that were initially recorded were used to generate 40 reference images that we will call vanilla. At the same time, these signals were then used as a basis for applying AWGN that differ in SNR. A limit SNR above which signal noise does not create images that are sufficiently different from the references was found empirically. Signals are noised with SNRs below the SNR limit and then new DIs are generated and batches of 40 (SP method) or 120 (RAPID method) noisy images are created per SNR value. We could generate 4 times more images for the RAPID method than for SP method because we could consider 4 subsets of sensor configurations: [1,2,3,4,5], [1,4,2], [2,4,5] and [2,3,5]. Images generated for the SP method and RAPID method with the noisy signals are shown in Figure 3.

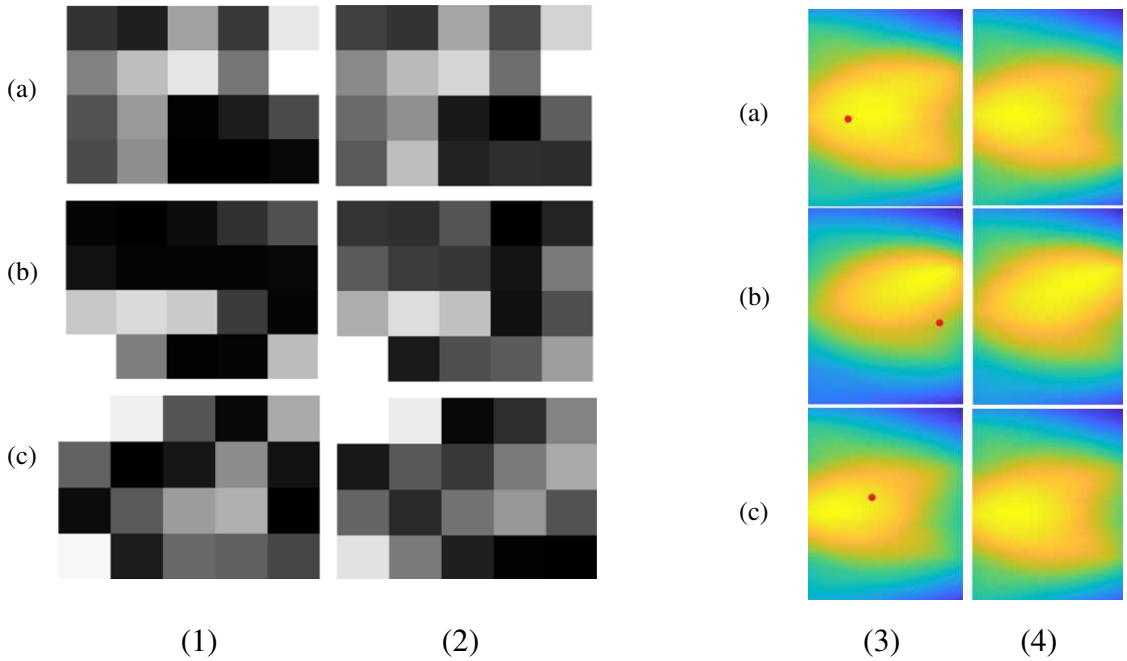

Figure 3. SP vanilla (1) vs. noisy (2) images with AWGN for SNR=50.5 dB and for the DI Welch-based Power Spectral Density (WPSD). Damage is by delamination (a), impact (b) and magnet (c). RAPID vanilla (3) vs. noisy (4) images with AWGN for SNR=30, for the 'CRC' DI and the [1,2,3,4,5] sensor configuration. Damages are by delamination (a), impact (b) and magnet (c). For each damage, the red point indicates the real damage location on the RAPID image.

For the SP method, it can be observed that according to the damage, the reference image and the artificially created AWGN image have the same structure and differ only in the light intensity of some pixel blocks. The main information in the artificial image, i.e., the white pixel that informs about the largest DI, is located at the same place and is of the same intensity as in the corresponding vanilla image. In a similar way to the SP images, it is observed here that the pixel maximum of the artificial RAPID images is located within a very small pixel radius compared to the reference images. The damage localization maps are broadly similar, some pixel protrusions are more pronounced in the artificial images, but the essential information of the position of the pixel maximum is common. After several batches for each method, we finally managed to generate 418 images per class for the SP method, i.e., 1254 images, and 460 images per class for the RAPID method, i.e., 1380 images.

Now that the image databases have been generated for these two methods, it is a question of moving on to the supervised learning stage in order to carry out a classification task, initially using neural networks created and learned from scratch, and then using an architecture database from the literature which has proved its worth and which will facilitate learning: the VGG16 network. Neural networks are increasingly used in the SHM literature because of their ability to autonomously inspect aging structures. Compared to traditional machine learning methods such as random forests, k-means or SVMs, the MLP-type networks can extract features from data to perform classification tasks. A perfectly trained network could be made to recognize damage classified into several classes without any human intervention. Despite the autonomy that this supervised learning method allows, one of the challenges is to optimize the computational time efficiently to perform SHM tasks. After flattening the features into a single vector in the last convolution layer, the fully connected hidden layer architecture of an MLP is involved. At the end of the last layer is an activation function, most often 'Softmax', which is

used to determine the probability of the input belonging to a class. Thus, CNNs have architectures that have the role of distinguishing classes of data with a 3D representation, which is very suitable for a case study of SHM. The first appearance of a CNN architecture was the LeNet-5, proposed by Le-Cun et al. It was then followed by VGG16 by Simonyan et al. [10]. The full CNN theory will not be studied here but is detailed in [11]. We shall focus on the CNN architecture chosen and the hyperparameters setting. In a first step, we worked with a learning architecture from scratch presented in Figure 4. This network is mainly composed of 3 convolution layers with the addition of max-pooling, a filtering and information reduction steps necessary for the network:

- C1: 32 filters 3x3 (activation='RELU', padding = 'SAME') + S2: max-pooling kernel 2x2 (padding='SAME', stride=2)
- C3: 32 filters 3x3 (activation='RELU', padding = 'SAME') + S4: max-pooling kernel 2x2 (padding='SAME', stride=2)
- C5: 32 filters 3x3 (activation='RELU', padding = 'SAME') + S6: max-pooling kernel 2x2 (padding='SAME', stride=2)

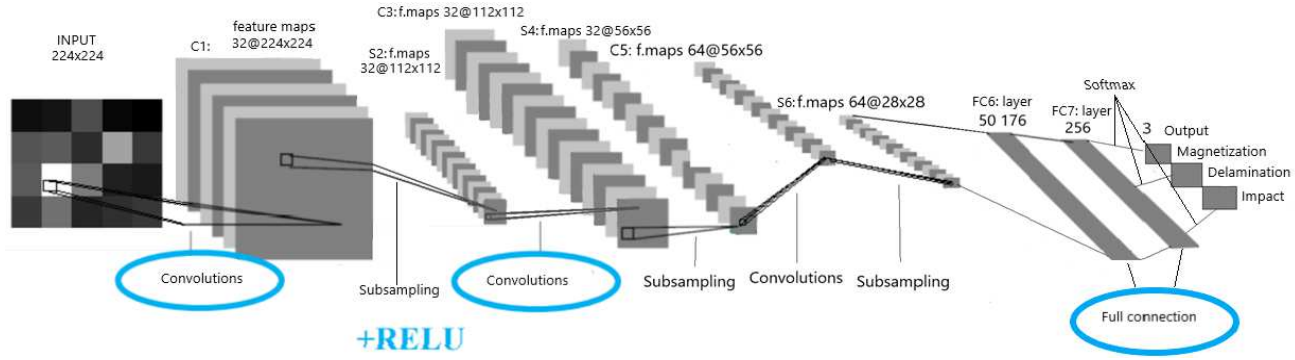

Figure 4. Architecture of the CNN with 224x22 SP images as input, with C: convolution layer, S: max-pooling sampling step, FC: fully connected layer.

The output of the S6 sampling layer is 64 feature maps of size 26x26. These feature maps characterize the elements of the image which define it in a unique way and allow it to be distinguished from other images. Their juxtaposition is used as input to a fully connected multi-layer neural network. This is done in a step called "flattening", where all the maps are flattened into vectors and then juxtaposed. Now that the images have been processed and formatted, their new format is suitable for performing a classification task via an MLP whose composition is as follows:

- FC6 (Fully connected) : 256 perceptrons (activation='RELU')
- FC7: 3 perceptrons (activation='SOFTMAX')

The activation function SOFTMAX is used to represent the categorical law obtained at the end of the network, we associate a score to each output possibility, which we transform into a probability with the function. After classification, a loss function must be placed to determine the classification accuracy deviation for a given iteration. We have chosen the cross-entropy function. The objective is to minimize the total prediction disorder with an algorithm that will update the weights of the network in such a way as to come as close as possible to a minimum of the loss function. This is achieved by a gradient descent algorithm whose efficiency can be influenced by changing the learning rate λ, the step of the algorithm.

2.3 Classification results

For each image generation method, the folders containing the images for each damage shall be loaded, processed, and fed into a CNN architecture that may be from scratch or already existing. The results that will be studied will draw the loss function over the epochs, as loss value implies how poorly or well a model behaves after each iteration of optimization, and the accuracy metric as it is a measure of how accurate the model's predictions are compared to the true data. We will also compare the two methods in terms of learning time, as the temporal resources are a major stake in SHM procedure. Two alternative methods that aim at reducing temporal cost and achieve better accuracy will be applied, one using only a MLP model for the SP method, and the other exploiting the classification power of the pre-trained VGG16 architecture for both methods. The Table 1 Summarizes the results in accuracy and loss for the SP and RAPID methods and the settings that were used for learning over several training sessions. The total numbers of images are of the same order of magnitude, which allows comparisons based on the accuracy results. 15 training sessions were conducted for each damage to raise the

Table 1. Results for the classification task for the two methods.

Method name	Total number of images	Number of training data	Number of test images	Epochs	Learning rate	Average loss	Average accuracy
Sensor placement	1254	1003	125	30	0.001	0.372	0.928
RAPID	1380	1104	138	30	0.01	0.915	0.511

average information depicted in table 1. We observe that for the three classes classification task, the results seem significantly better for SP method, even though both datasets are limited. For the same epoch number, i.e., the same allocated time for the network to configure weights, accuracy is close to 1 for SP method while it has never exceeded 0.6 accuracy for the RAPID images. However, we observe a relatively high loss with respect of that high accuracy for the SP images. This could be interpreted with the mathematical expression of the loss. When plotting a histogram of the loss function per samples, we notice that the loss is actually very low for most samples and there are few outliers with a consequent loss. Since the total loss is the average, we discern a high loss even though it is performing well on all but a few points. Optimal learning rate for RAPID method was found at 0.01 and used to conduct test. For the SP method, it was valued at 0.001. For the generation of the database, the generated images are quite large (656x875), as we wanted to keep as much information as possible for the RAPID images because, unlike the SP method images that could be reduced to 4x5 because the arrangement of pixels in the form of a grey level block can be used to form images of size number of pixel blocks in width times number pixel of blocks in height. It would no longer be necessary to use CNNs, but to go directly to the flattening stage as the images are no longer as complex. The training would only concern one MLP to significantly reduce the training time. The MLP results for SP method CNN results for RAPID method are shown in Figure 4.

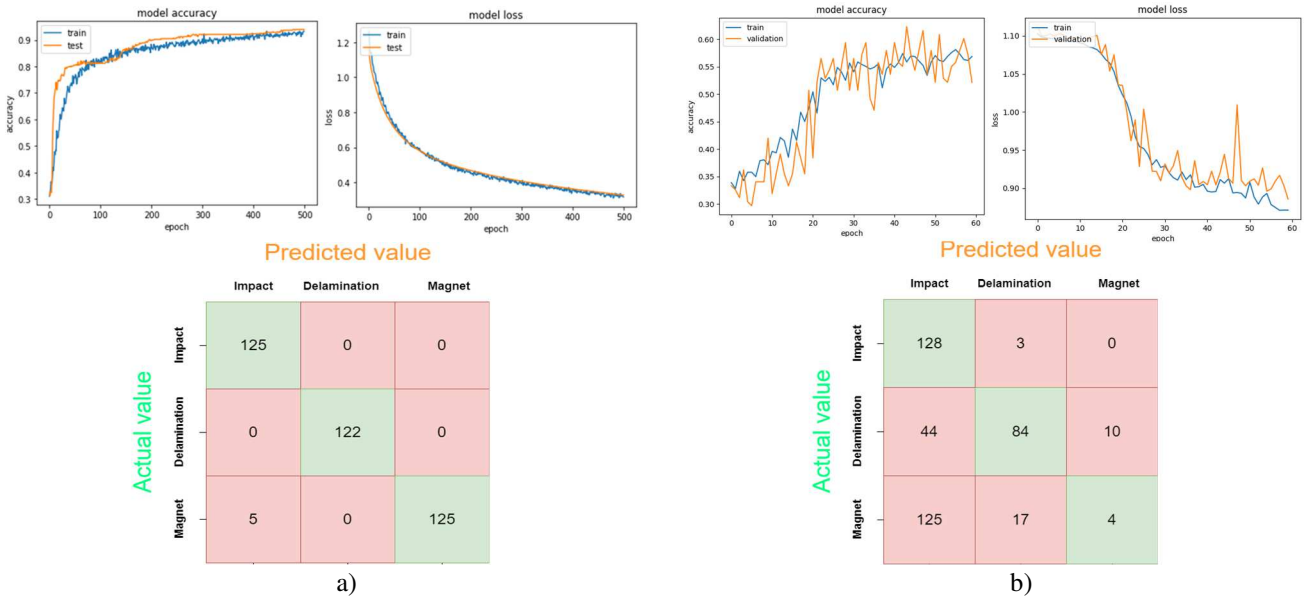

Figure 5. a) Performance of a MLP with the SP method for $\boldsymbol{\lambda = 0.001}$, epochs = 500 and confusion matrix after transfer learning is applied and b) CNN performance with RAPID images for $\boldsymbol{\lambda = 0.001}$, epochs = 60 and confusion matrix obtained for RAPID method after transfer learning is applied.

For the SP method, the accuracy is improved and the curves are smoothed. Correctly classified examples go up to 94%, which is at least a gain of 1% in accuracy compared to Table 1 results. Most importantly, the learning time is reduced by 60. Over multiple tests, we save a considerable amount of time compared to the convolution architecture that is here unnecessary. The network manages to minimize the classification error with a reduced image base in the order of a minute. For 60 epochs which gave the best results, accuracy is less satisfactory considering the RAPID method. For such a low

learning rate, the network seems to converge, but barely achieved only 48% accuracy. This could be explained by the lack of data that led to overfitting, thus poor accuracy. The need to gather a large labeled database to achieve strong results was not successfully achieved mainly because of extremely expensive computational cost. When using transfer learning to overcome this issue, we obtained a decreased loss and an increased accuracy leading up to 95% of correct classification compared to the zero trained network, in only 30 epochs. The SP images show to fit well for this kind of task that is not too complex. The network manages to class efficiently the three types of damage, with few examples misclassified for the magnet damage. When performing other iterations, this confusion is not steady, the other two classes may be subject to misclassification. For the RAPID method confusion matrix in (b), we notice that impact damage has the best accuracy among the different classes. When we look at the image datasets for the other images, they are very similar to the impact damages when especially looking for the image generated for the other subset sensor configurations. The very resemblance of the images' pixel envelopes to the impact class could be an explanation for both classes being classed as such.

3. CONCLUSION

In our study, we utilized a Structural Health Monitoring (SHM) technique that employs ultrasound generated by piezoelectric sensor arrays for the classification process. Specifically, we developed and compared two methods, namely the Sensor Placement (SP) and the RAPID method, based on their classification performance in a Convolutional Neural Network (CNN). The results showed that the SP method consistently outperformed the RAPID method in the classification task. We observed no evidence of overlearning, and the loss function consistently decreased on both the validation and training datasets. Despite the limited amount of available data, the network output achieved an accuracy of over 90% in most trials. However, images obtained using the RAPID method failed to adequately distinguish between image classes, and the classifier could not exceed 60% accuracy despite the high temporal and spatial complexity of execution and the variety of parameter sets used. These suboptimal results can be attributed to the limited amount of data and the fact that the RAPID method was developed for localization tasks, and thus may not be optimally suited for this type of SHM task. Further work will focus on assessing the generalization power of the SP method by studying additional damage cases on a different stiffened plate, including variations of the damages studied in this paper.

REFERENCES

[1] Worden, K.; Farrar, C. R.; Manson, G. & Park, G. "The Fundamental Axioms of Structural Health Monitoring" Proceedings: Mathematical, Physical and Engineering Sciences, The Royal Society, **2007***, 463*, 1639-1664

[2] Su, Z.; Ye, L. & Lu, Y. "Guided Lamb waves for identification of damage in composite structures: A review" Journal of sound and vibration, Elsevier, **2006***, 295*, 753-780

[3] Seventekidis, P.; Giagopoulos, D.; Arailopoulos, A.; Markogiannaki, O. Structural Health Monitoring using deep learning with optimal finite element model generated data. Mech. Syst. Signal Process. 2020, 145, 106972.

[4] Perfetto D., De Luca A., Perfetto M., Lamanna F. and Caputo F., Damage Detection in Flat Panels by Guided Waves Based Artificial Neural Network Trained through Finite Element Method. Materials 2021, 14, 7602.

[5] C. Efstathiades, C. C. Baniotopoulos, P. Nazarko, and L. G. E. Ziemianski, "Application of neural networks for the structural health monitoring in curtain-wall systems," Engineering Structures, vol. 29, no. 12, pp. 3475–3484, 2007.

[6] Yue, N.; Sharif-Khodaei, Z. Assessment of impact detection techniques for aeronautical application: ANN vs. LSSVM. J. Multiscale Modell. 2016, 7, 1640005.

[7] Nazih Mechbal, Marc Rébillat. Damage indexes comparison for the structural health monitoring of a stiffened composite plate. 8th ECCOMAS Thematic Conference on Smart Structures and Materials (SMART 2017), Jun 2017, Madrid, Spain. pp.436-444. ffhal-01592996

[8] William Briand, Lamb waves based active sparse tomography for damage size quantification in composite structures: data-driven and parameter inversion methods. Automatic. HESAM Université, 2022. English. ffNNT: 2022HESAE027ff. fftel-03676065.

[9] Xiaoliang Zhao, Huidong Gao, Guangfan Zhang, Bulent Ayhan , Fei Yan, Chiman Kwan and Joseph L Rose, *Active health monitoring of an aircraft wing with embedded piezoelectric sensor/actuator network: I. Defect detection, localization and growth monitoring,* Smart Materials and Structures 16 (4) (2007), p. 1208.

[10] Simonyan, K., Zisserman, A., "Very deep convolutional networks for large-scale image recognition", III. International Conference on Learning Representations (ICLR 2015), San Diego, USA, 1409– 1556, (2015).

[11] Tabian, I.; Fu, H.; Sharif Khodaei, Z. A Convolutional Neural Network for Impact Detection and Characterization of Complex Composite Structures. *Sensors* 2019, *19*, 4933. https://doi.org/10.3390/s19224933